Origin of the Catalytic Power of Acetylcholinesterase: Computer Simulation Studies

Monika Fuxreiter[†] and Arieh Warshel*[,‡]

Contribution from the Department of Theoretical Chemistry, Eötvös University, Budafest, Hungary, and Department of Chemistry, University of Southern California, Los Angeles, California 90089-1062

Received July 11, 1997[⊗]

Abstract: The energetics of the acylation step of AChE (acetylcholinesterase) is explored by using molecular simulation approaches. These include the evaluation of activation free energies by using the empirical valence bond (EVB) potential surface and an all-atom free energy perturbation (FEP) approach, as well as estimates of the catalytic effect of the enzyme by using the semimicroscopic version of the Protein Dipoles Langevin Dipoles (PDLD/S) method. The determination of the effect of the enzyme is based on the use of reliable experimental information in evaluating the energetics of the reference reaction in water and then on using robust simulations for the evaluation of the effect of moving the reacting system from a solvent cage to the protein active site. This procedure reduces the error range of the overall analysis since the energetics in water is not evaluated by a first principle approach. The use of two simulation methods and different initial conditions provide a way for assessing the error range of the calculations and the validity of the corresponding conclusions. Both the EVB and PDLD/S approaches show that the enzyme reduces the activation barrier of the acylation step by 10−15 kcal/mol relative to the corresponding reference reaction in water. This corresponds to a (10^7−10^{11})-fold rate acceleration, which is in good agreement with the corresponding experimental estimate. The origin of the catalytic power of the enzyme appears to be associated with electrostatic stabilization of the transition state. This electrostatic effect can be classified as a combination of reduction of the energy of the charged intermediate and reduction in the reorganization energy. The contributions of different protein residues to the stabilization of the transition state are estimated. It is demonstrated that, in contrast to some proposals, AChE and other enzymes do not work by providing a hydrophobic environment but rather a polar environment. This work concludes that the most important catalytic effects are associated with nearby residues rather than distant ionized residues. It is also concluded that the enzyme has evolved first to optimize the speed of the actual bond breaking/bond making chemical processes and only then to fine-tune the rate by optimizing the barrier for the diffusion step. Since the optimization of the chemical step involves more than 10 kcal/mol and the optimization of the diffusion step involves at most 1 or 2 kcal/mol, it appears that the possible acceleration of the diffusion step is a second-order effect. These conclusions are consistent with the available experimental studies.

1. Introduction

Acetylcholinesterase (ACHE) is a serine hydrolaze that terminates the impulse transmission at cholinergic synapses by rapid hydrolysis of the neurotransmitter acetylcholine. To accomplish this task the enzyme uses one of the highest rate constants known[1] ($k_{cat} = 1.6 \times 10^4$ s^{-1}). The effectiveness of AChE catalysis is also reflected by the $k_{cat}/K_M \approx 2 \times 10^8$ M^{-1} s^{-1},[1] which is close to the limit of diffusion controlled reactions. The solution of the X-ray structure[2] and many biochemical studies (e.g. refs 1 and 3) have offered the opportunity of a detailed molecular understanding of AChE catalysis.

The 3D structure of AChE from *torpedo californica* showed that the catalytic triad consists of Ser-200, His-440, and Glu-327 (Figure 1). This resembles the catalytic triad of serine proteases; however, Glu appears as the third residue instead of Asp. The replacement of any of these three residues by alanine causes loss of enzymatic activity.[4] It turned out that the catalytic triad is located at the bottom of a 20 Å deep gorge, which consists of a large number (14) of aromatic residues, which are highly conserved in AChE's from different species. Crystallographic studies on AChE complexing the transition state analog inhibitor TMTFA provided a detailed picture of the "esteratic" and "anionic" subsites forming the acyl and choline binding pocket,[5] whose presence was indicated by early kinetic studies.[6] The ammonium binding locus consists of Trp-84, Glu-199, and Phe-330, whereas the acyl binding pocket is formed by Trp-233, Phe-288, Phe-290, and Phe-331. Trp-84 has a close contact to the quaternary ammonium group (3.7 Å) playing an

* To whom correspondence should be addressed.
† Eötvös University.
‡ University of Southern California.
⊗ Abstract published in *Advance ACS Abstracts,* December 15, 1997.
(1) Rosenberry, T. L. *Adv. Enzymol. Relat. Areas Mol. Biol.* **1975**, *43*, 103.
(2) Sussman, J. L.; Harel, M.; Frolow, F.; Oefner, C.; Goldman, A.; Toker, L.; Silman, I. *Science* **1991**, *253*, 872.
(3) Quinn, D. M. *Chem. Rev.* **1987**, *87*, 955.
(4) Shafferman, A.; Velan, B.; Ordentlich, A.; Kronman, C.; Grosfeld, H.; Leitner, M.; Flashner, Y.; Cohen, S.; Barak, D.; Ariel, N. *EMBO J.* **1992**, *11*, 3561.
(5) Harel, M.; Quinn, D. M.; Nair, H. K.; Silman, I.; Sussman, J. L. *J. Am. Chem. Soc.* **1996**, *118*, 2340.
(6) Froede, H. C.; Wilson, I. B. In *The Enzymes*; Boyer, P. D., Ed.; Academic Press: New York, 1971; Vol. 5, p 87.

S0002-7863(97)02326-3 CCC: $15.00
Published on Web 01/14/1998

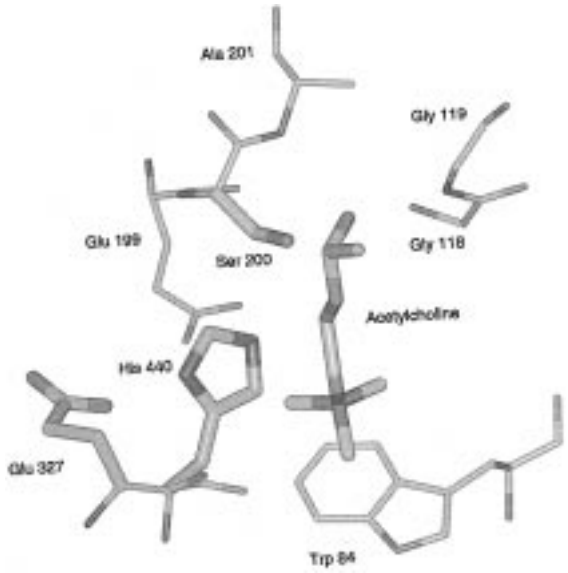

Figure 1. The substrate and key active site residues.

important role in substrate binding. This is also reflected by the nearly 1000-fold increase in the K_M of the W84A mutant compared to the K_M of the wild-type enzyme.[7] Glu-199 was assumed to contribute to the stabilization of the histidinium ion formed prior to the acylation step. Surprisingly, the E199Q mutant showed only a 5-fold decrease in k_{cat}[4,7] indicating that this residue does not play a major catalytic factor. The replacement of other residues (Phe-288, Phe-330, Phe-331) has only a slight effect on the rate of catalysis.[4,8]

On the basis of the model obtained by docking acetylcholine into the crystal structure of AChE,[2] it was suggested that an oxyanion hole is formed by the main chain N−H dipoles of Gly-118, Gly-119, and Ala-201, which interact with the carbonyl oxygen of the substrate. The structure of the AChE−TMTFA complex has also supported this hypothesis.[5]

Most of the effort in correlating the crystal structure of AChE with its action has been focused on the diffusion step (e.g. refs 9 and 10). However, the actual rate acceleration indicates that the enzyme must have evolved to catalyze a rather slow reaction by making it as fast as possible rather than just optimizing the diffusion rate. That is, the rate in enzyme is around 10^8 M^{-1} s^{-1} while the rate constant for OH^- attack an acetylcholine in water is 2.2 M^{-1} s^{-1}.[11] Thus (although the definition of the catalytic effect depends on the reference state) the enzyme does accelerate the hydrolysis of acetylcholine by more than 8 orders of magnitude by any reasonable definition. Since the most an enzyme can do in optimizing diffusion is around one order of magnitude rate acceleration, it appears that the enzyme has evolved mainly to catalyze the chemical step of the hydrolysis reaction. In view of this fact it is important to focus on the actual bond breaking/bond making "chemistry" of the enzyme in order to understand the origin of its catalytic power.

Instructive attempts for understanding the catalytic power of the enzyme by using mutation experiments were reported recently.[5] However, despite the insight provided by mutation experiments (e.g. ref 12), such studies cannot tell us in a conclusive way what is the origin of the overall catalytic effect of the enzyme. To realize this important point it is useful to think of a hypothetical nonpolar enzyme with a single hydrogen bond donor that stabilizes a negatively charged transition state. Mutation of this hydrogen bond will lead to an enormous reduction in the rate of the reaction and this may lead one to assume that the native enzyme is a good catalyst. However, the native enzyme will still be a very poor enzyme since its reaction will be much slower than the corresponding reaction in water (for a related illustration see Figure 3 of ref 13). Thus, it is important to relate the structure of AChE to its total catalytic effect. The present work addresses this challenge by using computer simulation approaches. This is done by using microscopic and semimicroscopic approaches to determine how the enzyme reduces the energy barrier of the acylation step of acetylcholine hydrolysis compared to the reference reaction in water.

2. Simulation Methods

Reliable simulations of enzymatic reactions are extremely challenging.[14] Thus it is crucial to have a clear estimate of the error range of the computational approaches used. Here we assess the accuracy of our calculations by using two different but complementary simulation approaches, the EVB/FEP and the PDLD/S methods. These methods will be outlined below.

2.1. EVB/FEP Simulations. The EVB method has been discussed extensively elsewhere (e.g. refs. 15 and 16), thus we mention here only the points which are most relevant to the present study. The EVB model treats each reaction step as a transition between different valance bond (VB) configurations or resonance structures. Each of these states is modeled by a molecular mechanics force field, whereas the actual quantum mechanical ground state is obtained by mixing a VB configurations. The EVB method can be incorporated into the free energy perturbation (FEP)/umbrella sampling method that allows one to evaluate the free energy surface of each reaction step. The EVB surface can be calibrated against experimental data for relevant reactions in water and on theoretical studies of gas phase reactions. This guarantees the correctness of the energetics of the reference reaction in water. Consequently, the reliability of the calculated catalytic effect depends primarily on the difference between the reaction in enzyme compared to the reference reaction. In the present case we describe the reaction by three resonance structures depicted in Figure 2; the relevant charges are presented in Table 1 (the table contains two charge sets for stability tests). The EVB Hamiltonian involves diagonal and off-diagonal terms. The diagonal elements of the EVB Hamiltonian correspond to the energy of each resonance structure and are given by (e.g. ref 16)

$$E_i = H_{ii} = \sum_j \Delta M_j^{(i)}(b_j^{(i)}) + \frac{1}{2}\sum_l \gamma_l^{(i)} k_l^{(i)}(\theta_l^{(i)} - \theta_{0,l}^{(i)})^2 + V_{nb,rr}^{(i)} + \alpha^{(i)} + V_{nb,rs}^{(i)} + V_s \quad (1)$$

where $\Delta M_j^{(i)}$ denotes the Morse potential (relative to its minimum value) for the jth bond in the ith VB structure. The second and third terms, respectively, denote the bond angle bending contribution and the nonbonded electrostatic and van der Waals interactions between

(7) Ordentlich, A.; Barak, D.; Kronman, C.; Ariel, N.; Segall, Y.; Velan, B.; Shafferman, A. *J. Biol. Chem.* **1995**, *270*, 2082.
(8) Ordentlich, A.; Barak, D.; Kronman, C.; Flashner, Y.; Leitner, M.; Segall, Y.; Ariel, N.; Cohen, S.; Velan, B.; Shafferman, A. J. *Biol. Chem.* **1993**, *268*, 17083.
(9) Ripoll, D. L.; Faerman, C. H.; Axelsen, P. H.; Silman, I.; Sussman, J. L. *Proc. Natl. Acad. Sci. U.S.A.* **1993**, *90*, 5128.
(10) Tan, R. C.; Truong, T. N.; McCammon, J. A.; Sussman, J. L. *Biochemistry* **1993**, *32*, 401.
(11) Wright, M. R. *J. Chem. Soc. B* **1968**, 545.
(12) Mildvan, A. S.; Weber, D. J.; Kuliopulos, A. *Arch. Biochem. Biophys.* **1992**, *294*, 327.
(13) Warshel, A.; Papazyan, A. *Proc. Natl. Acad. Sci. U.S.A.* **1996**, *93*, 13665.
(14) Náray-Szabó, G.; Fuxreiter, M.; Warshel, A. In *Computational Approaches to Biochemical Reactivity*; Náray-Szabó, G., Warshel, A., Eds.; Kluwer Academic Publishers: The Netherlands, **1997**; p 237.
(15) Warshel, A. *Computer Modeling of Chemical Reactions in Enzymes and Solutions*; John Wiley & Sons: New York, 1991.
(16) Åqvist, J.; Warshel, A. *Chem. Rev.* **1993**, *93*, 2523.

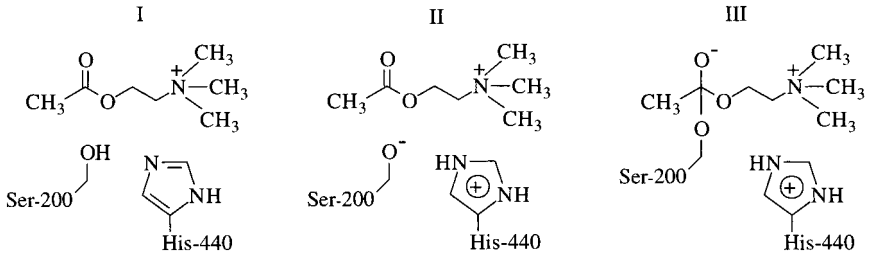

Figure 2. Resonance structures used in the EVB model to simulate the acylation step of acetylcholine hydrolysis. Resonance structures I, II, and III correspond respectively to the reactants, the state formed after the proton transfer step, and the tetrahedral intermediate state.

Table 1. Atomic Charges Used for EVB Resonance States[a]

residue	atom	I	II	III	III (ab initio)
Ser 200	CB	−0.100	−0.100	−0.100	−0.093
	HB1	0.050	0.050	0.050	0.100
	HB2	0.050	0.050	0.050	0.101
	OG	−0.450	−1.00	−0.159	−0.360
	HG	0.450	0.000	0.000	0.000
His 440	CG	0.035	0.160	0.160	0.160
	ND1	0.013	−0.160	−0.160	−0.160
	HD1	0.187	0.190	0.190	0.190
	CE1	0.110	0.540	0.540	0.540
	HE1	0.077	0.070	0.070	0.070
	NE2	−0.550	0.030	0.030	0.030
	CD2	0.058	0.100	0.100	0.100
	HD2	0.070	0.070	0.070	0.070
substrate	C3	−0.273	−0.273	−0.273	−0.170
	H31	0.114	0.114	0.114	0.055
	H32	0.125	0.125	0.125	0.009
	H33	0.113	0.113	0.113	0.024
	C2	0.248	0.248	0.248	0.291
	O6	−0.159	−0.159	−1.00	−0.617
	O5	−0.266	−0.266	−0.266	−0.322
	C4	−0.023	−0.023	−0.023	0.031
	H41	0.104	0.104	0.104	0.097
	H42	0.107	0.107	0.107	0.040
	C8	−0.052	−0.052	−0.052	0.009
	H81	0.129	0.129	0.129	0.075
	H82	0.134	0.134	0.134	0.098
	N11	−0.134	−0.134	−0.134	−0.213
	C7	−0.153	−0.153	−0.153	−0.060
	H71	0.144	0.144	0.144	0.118
	H72	0.146	0.146	0.146	0.091
	H73	0.145	0.145	0.145	0.124
	C10	−0.158	−0.158	−0.158	−0.059
	H01	0.146	0.146	0.146	0.092
	H02	0.145	0.145	0.145	0.129
	H03	0.144	0.144	0.144	0.120
	C9	−0.159	−0.159	−0.159	−0.097
	H91	0.146	0.146	0.146	0.112
	H92	0.143	0.143	0.143	0.144
	H93	0.144	0.144	0.144	0.132

[a] The EVB treatment included all the indicated fragments. The table contains two sets of charges. The first set is given in the first three columns whereas the second set is given in the first, second and fourth columns. The atom indexes correspond to the PDB notation.

the reacting groups (denoted by subscript *r*). The factor $\gamma_l^{(i)}$ in the second term is a coupling between bonds that are being broken or formed and those angles that depend on these bonds. The term $\alpha^{(i)}$ is the gas-phase energy of the *i*th state when all the fragments are at infinite separation. The nonbonded interaction with the surrounding protein and solvent, denoted by subscript s, is given by $V_{nb,rs}^{(i)}$. The last term (V_s) represents the internal potential energy of the protein/solvent system. The solute−solvent and solvent−solvent interactions are evaluated with the all-atom ENZYMIX force field[17] with the special SCAAS boundary conditions.[17] The off-diagonal elements of the Hamiltonian are represented by a simple single exponential approximation

$$H_{ij} = A_{ij} \exp\{-\mu r\} \tag{2}$$

where *r* is the distance between atoms whose bonding is changed upon transfer from state *i* to state *j*. The parameters A_{ij} and μ can be adjusted to reproduce the observed barrier for the reaction in solution or to reproduce gas-phase ab initio calculations. The actual ground state potential surface E_g is obtained by diagonalizing the EVB Hamiltonian (see ref 15 for a detailed discussion).

The EVB free energy is evaluated by driving the system from the reactant to the product state by using a mapping potential of the form

$$E_m = \sum E_i \eta_i^m \tag{3}$$

where η is changed by fixed increments (here we use η rather than λ to prevent confusion with the reorganization energy, and consider η as a vector with several components[18]). The data generated during this simulation are used to evaluate the reaction free energy $\Delta g(X)$, using a combination of the FEP and umbrella sampling approaches (see ref 15 for details) that gives

$$\exp[-\beta \Delta g(X')] = \exp[-\beta \Delta G\,(\eta_0 \rightarrow \eta_m)] \times \langle \delta(X - X') \exp[-\beta(E_g - E_m)] \rangle_{E_m} \tag{4}$$

where $\beta = 1/k_B T$, is the Boltzmann constant, η_m is the value of η that keeps the system closest to X', and $\langle\,\rangle_{E_m}$ designates an average over the trajectory with the given E_m. $\Delta G(\eta_0 \rightarrow \eta_m)$ is the free energy associated with changing the mapping potential from E_0 to E_m. This value is obtained by a standard FEP approach.[15]

The reaction coordinate *X* is taken usually (e.g. ref 15) as the difference between the values of the two EVB potentials that change during the given mapping step (e.g. $X = E_2 - E_1$ when we change η_1 and η_2).

The relevant activation barrier $\Delta g^{\ddagger}$ is obtained by $\Delta g^{\ddagger} = \Delta g(X^{\ddagger}) - \Delta g(X_0)$, where X_0 and $X^{\ddagger}$ are the values of the reaction coordinate at the ground and transition state, respectively. Previous EVB studies (e.g. ref 18) have demonstrated that it is possible to obtain a reasonable approximation for the change of $\Delta g^{\ddagger}$ upon transfer from water to the protein active site by considering only the intermolecular interactions between the substrate and its surroundings in evaluating eq 4, while still using the trajectories obtained with the full mapping potential. That is, one can evaluate

$$\exp[-\beta \Delta g(X')_{inter}] = \exp[-\beta \Delta G^{inter}\,(\eta_0 \rightarrow \eta_m)] \times \langle \delta(X - X') \exp[-\beta(E_{inter} - E_m^{inter})] \rangle_{E_m} \tag{5}$$

where the index "inter" designates the corresponding intermolecular contribution to ϵ and *E*. After evaluating $\Delta g(x^{\ddagger})_{inter}$ one can use the approximation

$$(\Delta\Delta g^{\ddagger})^{w \rightarrow p} \cong (\Delta\Delta g^{\ddagger})_{inter}^{w \rightarrow p} = (\Delta g_{inter}^{\ddagger})^p - (\Delta g_{inter}^{\ddagger})^w \tag{6}$$

This "electrostatic mapping" approximation reflects the fact that the intramolecular contributions to the overall free energy are quite similar

(17) Lee, F. S.; Chu, Z. T.; Warshel, A. J. *Comp. Chem.* **1993**, *14*, 161.

(18) Hwang, J.-K.; King, G.; Creighton, S.; Warshel, A. J. *Am. Chem. Soc.* **1988**, *110*, 5297.

in the solution and the enzyme cases. The evaluation of eq 5 converges much faster than that of eq 4 since it avoids the pathological instabilities that can occur when the E_i used in the mapping potential of eq 4 are very different from each other (this is a well-known phenomenon in FEP calculations, which occurs when the mapping potential E_m changes abruptly). For example, the energy contribution of the O···C bond that is being formed during the nucleophilic attack step is drastically different in E_2 and E_3 (it changes from a nonbonded to a Morse potential) and its evaluation involves significant instability at the mapping step where the vector (η_1, η_2, η_3) changes from (0, 1, 0) to (0, 0.9, 0.1). Thus we will focus here on evaluating the "intermolecular" or "solvation" energy contribution to $(\Delta\Delta g^{\ddagger})^{w\rightarrow p}$. The convergence of the calculations is assessed by comparing different sets of simulations with different simulation times.

One of the most crucial aspects of the EVB procedure is the parametrization of the reference reaction in water and particularly the determination of the relevant α's by forcing the energetics of the simulated solution reaction to reproduce the corresponding experimental (or high-level ab initio) results. The relevant ΔG and $\Delta g^{\ddagger}$ values used in parametrizing the solution reaction are discussed in detail in Sections 3.1 and 3.2.

Finally the effectiveness of the EVB method is evident from the fact that several research groups have recently adopted it for studies of chemical reactions in solutions and enzymes.[19−22]

2.2. PDLD/S Simulations. In addition to the EVB method one can estimate the catalytic effect of the enzyme by the semimicroscopic version of the PDLD model (see refs 17 and 23). This approach, which is referred to as the PDLD/S method, considers the protein as a medium with a "dielectric constant", ϵ_{in}, that represents all the contributions which are not treated explicitly (see below) and considers thermodynamic cycles where the dielectric constant of the solvent (water) is changed from its actual value, ϵ_w, to ϵ_{in}. The PDLD/S free energies for individual protein configurations are treated in the framework of the Linear Response Approximation (LRA),[24−27] which takes into account consistently the effect of protein reorganization in different steps of the binding cycle. This treatment leads, after a somewhat involved derivation,[27] to the following expression:

$$\Delta G_{bind} \cong [\langle \Delta G_{sol}^{l+p} \rangle - \langle \Delta G_{sol}^{p} \rangle - \langle \Delta G_{sol}^{l} \rangle_{Q=Q_0}]\left[\frac{1}{\epsilon_{in}} - \frac{1}{\epsilon_w}\right] + \langle V_{Q\mu} \rangle \frac{1}{\epsilon_{in}} + \Delta G_{hyd} + \Delta G_{vdw} - T\Delta S' + \Delta G_{relax} \quad (7)$$

here we use the notation

$$\langle \Delta G_{sol} \rangle = \frac{1}{2}[\langle \Delta G_{sol} \rangle_{Q=Q_0} + \langle \Delta G_{sol} \rangle_{Q=0}] \quad (8)$$

where p and l designate protein and ligand (substrate), respectively. ΔG_{sol} is the solvation free energy of the indicated system, evaluated by the microscopic (unscaled) PDLD method. Q is the charge distribution of the substrate atoms, which changes in our binding cycle (see ref 21) between the actual charge distribution (Q_0) and zero. $\langle\ \rangle_Q$ designates an average over the configurations generated with MD simulations with the designated Q. $V_{Q\mu}$ is the vacuum interaction between the charges to the ligand and the residual charges of the protein. ΔG_{hyd} is a field-dependent hydrophobic term (that estimates the relevant surface area from the number of Langevin dipoles in the first "solvation shell" and then corrects it by considering the local field on each dipole). ΔG_{vdw} is the van der Waals contribution to the bonding cycle, $\Delta S'$ is the contribution associated with the change in rotational and translational entropy of the uncharged ligands upon binding, and ΔG_{relax} represents the free energy associated with the relaxation of the uncharged ligand upon moving from the protein to water. The parameter ϵ_{in} represents, as stated above, the contributions that are treated implicitly and is not related directly to the actual "dielectric constant" of the protein (see discussion of refs 28 and 29). When the protein reorganization energy is taken into account explicitly it is usually reasonable to use $\epsilon_{in} \leq 4$ (see refs 23 and 29).

The calculation of the catalytic effect by the PDLD/S approach involves the evaluation of the binding energy in the ground and transition state using

$$(\Delta\Delta g^{\ddagger})^{w\rightarrow p} = (\Delta G_{bind}^{\ddagger} - \Delta G_{bind}^{0})^{w\rightarrow p} \quad (9)$$

where $\Delta G_{bind}^{\ddagger}$ and ΔG_{bind}^{0} designate the binding energy of the transition and ground state, respectively.

The average of eq 8 for the ground and transition states is obtained by using a central force field whose minimum energy structure is similar to that of the corresponding EVB surface. The relevant charges of the central force field are taken as the corresponding EVB charges.

In studies of enzymatic reactions it is useful to evaluate the effects of mutations of different residues. To perform such studies in a conclusive way it is essential to simulate the thermodynamic process that corresponds to each mutation. However, such calculations are quite expensive, and it is frequently useful to evaluate "group contributions" that correspond to the process of mutating the given residues to their fully nonpolar form (zero residual charges). A reasonable approximation for these contributions sometimes can be obtained by the so called "nonrelaxed" approximation.[26] This approximation only considers the $V_{Q\mu}/\epsilon_{in}$ term of eq 4. This seemingly oversimplified approach is quite effective if one uses a large ϵ_{in} (i.e. $\epsilon_{in} \approx 40$) for ionized residues and $\epsilon_{in} \sim 4$ for non-ionized residues (see ref 29). This and related approaches can be quite effective in screening for residues whose mutation can lead to significant effects.[26,27]

The EVB/FEP calculations and configuration generation for the PDLD/S calculations were performed with the program ENZYMIX.[17] The PDLD/S calculations were performed with the program POLARIS.[17]

3. Results and Discussion

3.1. Analysis of the Experimental Information for the Reaction in Solution and in Enzyme. Before summarizing and analyzing the actual calculations it is crucial to consider the experimental information about the reaction and to define the proper reference state. This step of the analysis (which is not yet taken by most practitioners in the field) is quite important as it helps to define the meaning of the catalytic effect in clear terms. There are several ways to select a reference state for enzymatic reactions, and some of them that involve effective concentration turn out not to be so useful when one is interested in well-defined energy considerations (the effect of concentration can always be considered after the energetics is known[15]). A useful definition of the catalytic effect can be obtained when one compares k_{cat} for the hydrolysis of acetylcholine by water $\sim 8 \times 10^{-10}$ s^{-1}; (e.g. see ref 30) to k_{cat} in the enzyme active site $\sim 1.6 \times 10^{4}$ s^{-1}; (e.g. see ref 1). By this definition we have a rate enhancement of 2×10^{13}. Considering the attack of OH^- on acetylcholine is more problematic. That is, in this case the reaction in water has a second-order rate constant of 2.2 M^{-1} s^{-1} (see ref 30), but this rate constant does not reflect

(19) Kim, H. J.; Hynes, J. T. J. *Am. Chem. Soc.* **1992**, *114*, 10508.
(20) Bursulaya, B. D.; Zichi, D. A.; Kim, H. J. *J. Phys. Chem.* **1996**, *100*, 1392.
(21) Bala, P.; Grochowski, P.; Lesyng, B.; McCammon, J. A. *J. Phys. Chem.* **1996**, *100*, 2535.
(22) Lobaugh, J.; Voth, G. A. J. *Chem. Phys.* **1996**, *104*, 2056.
(23) Sham, Y. Y.; Chu, Z. T.; Warshel, A. *J. Phys. Chem. B* **1997**, *101*, 4458.
(24) Lee, F. S.; Chu, Z. T.; Bolger, M. B.; Warshel, A. *Protein Eng.* **1992**, *5*, 215.
(25) Åqvist, J.; Medina, C.; Samuelsson, J.-E. *Protein Eng.* **1994**, *7*, 385.
(26) Muegge, I.; Schweins, T.; Langen, R.; Warshel, A. *Structure* **1996**, *4*, 475.
(27) Muegge, I.; Tao, H.; Warshel, A. *Protein Eng.* In press.
(28) King, G.; Lee, F. S.; Warshel, A. *J. Chem. Phys.* **1991**, *95*, 4366.
(29) Muegge, I.; Qi, P. X.; Wand, A. J.; Chu, Z. T.; Warshel, A. *J. Phys. Chem. B* **1997**, *101*, 825.
(30) Schowen, R. L. In *Transition States of Biochemical Processes*; Gandour, R. D., Schowen, R. L., Eds.; Plenum: New York, **1978**; p 77.

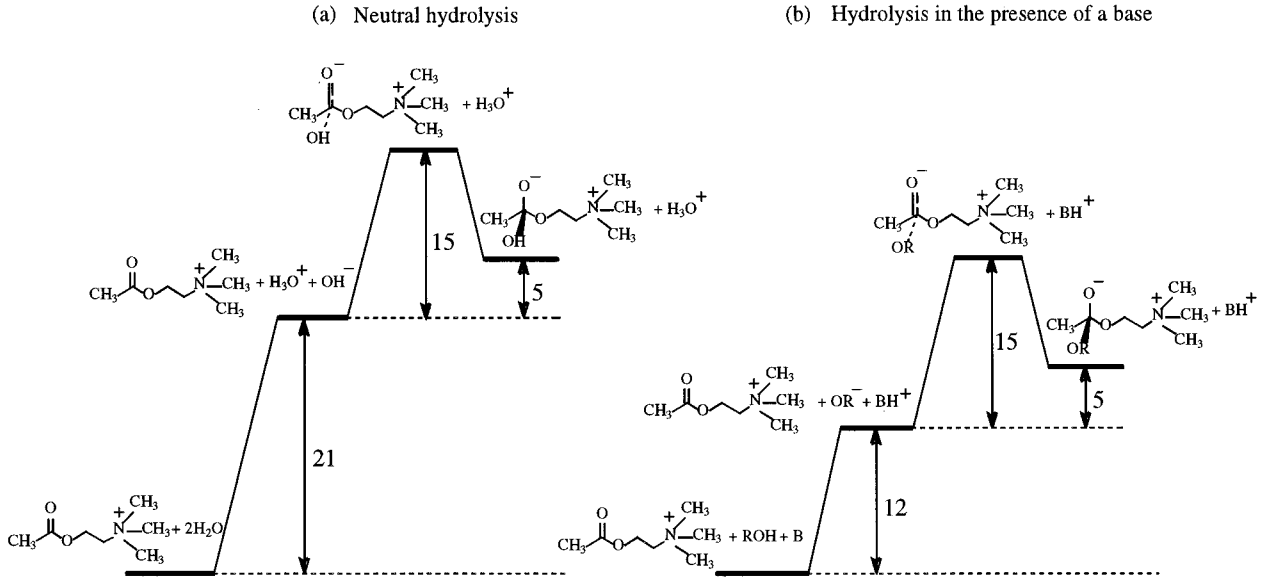

Figure 3. Experimentally based estimates of the energetics of acetylcholine hydrolysis in a solvent cage (a) with water as a base and (b) with histidine as a base.

the energetics of the formation of the OH^- ion. At any rate, just obtaining the rate enhancement does not help so much in finding its origin. In our experience the most unique way of analyzing the effect of the enzyme is obtained by relating rates to free energies. This becomes particularly true when one compares the reaction in the enzyme to a reference reaction in a water cage that involves the *same* mechanism as that *assumed* for the enzyme.[15] In such a case we eliminated the need to consider the rather trivial (yet confusing) entropic effect of bringing the reactants to close proximity (see discussion in ref 15). Before comparing the energetics of the enzyme reaction to the proper reference reaction let us start by illustrating our approach of analyzing the energetics in solvent cages. This will be done by considering the above mentioned neutral hydrolysis (Figure 2). In our analysis we assume (see below) that this reaction is a stepwise process of the proton transfer between two water molecules and a nucleophilic attack of the OH^- on the carbonyl of the acetylcholine molecule. The first step can be described as

$$2H_2O \rightarrow (H_3O^+)_{aq} + (OH^-)_{aq} \qquad (10)$$

The free energy of this reaction for two water molecules that are in contact with the substrate is ∼21 kcal/mol according to the considerations of footnote 31. The energetics of the nucleophilic attack step can be assessed from the rate constant for OH^- attack on acetylcholine, which is 2.2 M^{-1} s^{-1}. In converting this value to the relevant free energy in a solvent cage, we have to ask what will be the rate constant once the OH^- is in the same cage as the substrate. In such a case we have to consider the rate constant at 55 M OH^-. Using 2.2 × 55 s^{-1} and absolute rate theory, one obtains an activation barrier of ∼15 kcal/mol. Of course, the attack by a methoxy ion would be the best reference reaction in water, but no experimental data were available for this reaction. As in the case of other systems we assume that the rate constants for hydrolysis by an hydroxide and by a methoxy ion are of the same order of magnitude. Thus we use in our analysis the experimental data on hydrolysis by an hydroxide ion. Combining these results gives the energetics depicted in Figure 3a, and an overall barrier of ∼36 kcal/mol. This value is somewhat higher than the barrier deduced from the observed rate constant of the neutral reaction in water (∼30 kcal/mol). However, the 36 kcal/mol estimate reflects an assumed stepwise mechanism where the free energy is evaluated along the corners of the two-dimensional free energy diagram (defined by the length of the oxygen−hydrogen bond and the oxygen−carbon bond that are being broken and formed, respectively, during the reaction). The actual reaction coordinate might be more concerted and have a somewhat lower activation barrier. Nevertheless, the 36 kcal/mol value provides a quantitative estimate for the energetics of a stepwise mechanism in water, and this estimate is relevant to the energetics of an assumed stepwise mechanism in the enzyme. We expect that the effect of the enzyme on a stepwise mechanism is strongly correlated with its effect on a more concerted mechanism,[15] or in other words that a similar catalytic effect is obtained for both mechanisms. It is important to note that our results are consistent with the related analysis of Schowen[30] who used different considerations.

While the analysis of the neutral reaction in water is useful it is not fully relevant to the catalytic effect of the enzyme. For example the reaction in enzyme involves a histidine base rather than a water molecule and a serine ion rather than OH^-. Of course, one can view the use of different chemical reagents as the catalytic effect but this is not so useful. Thus it is more instructive to consider a reference reaction that involves the same reactants as the corresponding enzymatic reaction and to define, for example, the effect of changing the base as *a "chemical"*

(31) The relevant free energy in a solvent cage can be estimated as follows. First, we estimate the free energy of this reaction in an hypothetical solution with 1 M H_2O, 1 M OH^-, and 1 M H_3O^+. The corresponding ΔG_0 is obtained by the relationship $G_0 = RT \ln K_{eq} = RT \ln (10^{-14}/55^2) =$ 24.0 kcal/mol. Next, we change this ΔG_0 to the corresponding free energy when the water concentration is 55 M, which gives $\Delta G = \Delta G_0 + RT \ln Q = 24 - RT \ln 55^2 = 19.2$ kcal/mol (where $Q = [OH^-][H_3O^+]/[H_2O]^2$ in the given assumed nonequilibrium conditions with 1 M of OH^- and H_3O^+ and 55 M H_2O). Now we ask how much we have to pay for moving OH^- and H_3O^+ from their molar volume to the relevant solvent cage of, say, the size of one water molecule in the proper place near the substrate. This free energy is given approximately by $RT \ln(55^2) = 4.8$ kcal/mol (see problem 5.1 in ref 15). Now the free energy of the reaction in a solvent cage is ∼24 kcal/mol. However, we should also take into account the electrostatic interaction between OH^- and H_3O^+ in water, which can be estimated quite accurately by using Coulomb's law with a dielectric of ∼30 and is approximately 2.5 kcal/mol (see ref 55). This gives $\Delta G \cong 21.5$ kcal/mol based on purely experimental and thermodynamic considerations.

rather than catalytic factor. This is justified since the chemical effect of changing the intrinsic pK_a of the base has never been a really challenging puzzle in studies of enzymatic catalysis. At any rate, considering the same reactants in the enzyme and in the reference reaction leads to the energetics depicted in Figure 3b. Now the energy of the proton transfer step is given by

$$\Delta G^{w}_{PT} = 1.38(\mathrm{p}K^{w}_{a}(\mathrm{Ser}) - \mathrm{p}K^{w}_{a}(\mathrm{His})) \approx 12\mathrm{kcal/mol} \qquad (11)$$

We also assume that the energetics of the nucleophilic attack step is similar for OH^- and Ser^- (see discussion below). Thus, the overall activation barrier for our reference reaction in water is $(\Delta g^{\ddagger}_{cage})^{w} \sim 27$ kcal/mol. If we consider a possible overestimate for the activation barrier of the nucleophile attack in a stepwise mechanism (the above mentioned difference between our estimate of 36 kcal/mol and the observed barrier of ~30 kcal/mol for the neutral reaction) we obtain a lower limit of $(\Delta g^{\ddagger}_{cage})^{w} > 21$ kcal/mol.

Our preliminary analysis of the available kinetic information about the hydrolysis of acetylcholinesterase (ref 32) indicated that the deacylation step involves the highest barrier in the overall free energy profile. However, considering the activation barrier for each step relative to its own ground state rather than relative to the E + S state, we find $\Delta g^{\ddagger}$ of ~12 and 11.8 kcal/mol for the deacylation and acylation steps, respectively (the corresponding k_2 and k_3 are 2.5×10^4 and 1.6×10^4 s^{-1}, respectively[33]). Considering the above estimate of ~27 kcal/mol for the stepwise mechanism in our reference solvent cage, we find that the enzyme must reduce the barrier for the acylation step by $27 - 11.8 \sim 15$ kcal/mol. If we use our lower limit we obtain $\Delta\Delta g^{\ddagger} > 21 - 11.8 > 10$ kcal/mol. Thus, in dealing with the acylation step, we have to account for *at least* a (1.73×10^7) to (1.4×10^{10}) rate acceleration.

It should be emphasized at this point that the above analysis serves for more than just estimating the effect of the enzyme. That is, the energetics of the stepwise mechanism provide a quantitative way of calibrating the EVB potential and allows one to focus on the effect of the enzyme on a well-defined reaction coordinate whose energetics is usually correlated with the energetics of the actual mechanism even if the mechanism is concerted.[15]

3.2. EVB/FEP Calculations. The starting point for our simulation study was the crystal structure of TcAChE.[2] The original coordinates were prepared for the simulation runs in the following way: (i) Residues beyond 20 Å from the carbonyl carbon of the substrate were trimmed to "super atoms" and constrained by using the standard ENZYMIX protocol.[17] The only residue (Lys 325) within 20 Å that was incomplete in the crystal structure was built into the sequence and relaxed (the numbering of residues corresponds to AChE *torpedo californica*). Hydrogen atoms and water molecules were generated by the ENZYMIX program, instead of using the crystallographic water molecules. This approach, which is part of our standard simulation approach (dating back to ref 34), is fully justified since X-ray studies only provide information about rather few solvent molecules, and this is usually done for only one state of the reacting system. Of course, the simulations allow the solvent molecules to properly relax in and around the active site and to reorient upon changes of the reacting system. (ii) The enzyme was then subjected to 10000 relaxation steps at 30 K, using 0.5 fs time steps and a weak (0.03 kcal/(mol^{-1} Å^{-2})) internal protein constraint (a constraint that keeps the protein atoms close to the observed X-ray structure).

As stated in the method section we focus here on the intermolecular contribution to the *change* in the activation barrier $(\Delta\Delta g^{\ddagger})^{w\rightarrow p}$ rather than on the total contribution to this change. The validity of this approximation is demonstrated in ref 18. To evaluate this $(\Delta\Delta g^{\ddagger})^{w\rightarrow p}_{inter}$ we run a series of simulations for the two reaction steps in water and in the protein. This involves 20−40 ps molecular dynamics (MD) trajectories, changing the mapping parameters η_1, η_2, η_3 from (1.0, 0.0, 0.0) to (0.0, 0.0, 1.0) in 40 to 20 steps, respectively. The first 10% of the data at each η point was discarded in the evaluation of the free energy profile. The simulations were carried out at 300 K with an MD step size of 1 fs. The calculations were performed with the spherical SCAAS model[35−36] with its consistent polarization constraints. The center of the SCAAS system was taken at the C2 atom of the substrate, and the sphere radius was taken as 22 Å. The protein−protein and water−water interactions were treated by using the Local Reaction Field (LRF) method,[37] which provides accurate treatment of the long-range effects. This corresponds to having no cutoff in the first step after updating the nonbond interaction and having an extremely good approximation for the no-cutoff result in subsequent time steps (see ref 37). The forces associated with induced dipoles of the system were considered in all calculations. The error bar for the simulations was assessed by running the trajectories with different initial conditions and for a different length of time (see below).

The α's of the EVB potentials were adjusted to values that forced the calculated free energies of the solution reaction to reproduce the energetics of Figure 2b. The EVB parameters are those used before in simulating serine proteases[18] with the exception of the residual charges of Table 1. This table gives two sets of "solute" charges; The first is a standard EVB set (set 1), and a second set (set 2) where the charges of the tetrahydral intermediate state (state III) are taken from an ab initio Mulliken population analysis with a single point HF and a minimal basis set. The ester carbonyl system was treated in the same way as the amide carbonyl group of subtilisin,[12] and the "chemical" difference between the amide and ester systems was taken into account by using different α's. Here we focus on a qualitative treatment using the electrostatic mapping of eq 5, and the corresponding α's were taken as 101 and 29 kcal/mol, respectively, for the proton transfer and nucleophilic attack steps. The parameters of A_{12} and A_{23} of eq 2 were taken as 20 and 36 kcal/mol for these two steps, respectively, with $\mu = 0$ in both cases. This simplification of eq 2 was found to be a reasonable approximation for the electrostatic mapping approach.

Since the ΔG_0 for the nucleophilic attack step in water is not available from direct experimental studies, we estimated it by ab initio calculations of attack of a methoxy ion on methyl acetate in aqueous solution. The geometry of this system in both reactant and product (tetrahedral intermediate) state was optimized in the gas phase, using the 4-31G* basis set. The energy of the optimized geometries was calculated by MP2 single point calculation, using the 6-31G** basis set. The charges for the solvation energy calculation were obtained by the PCM method,[38,39] using 6-31G* basis set. The solvation

(32) Fuxreiter, M.; Warshel, A. Unpublished Results.
(33) Froede, H. C.; Wilson, I. B. *J. Biol. Chem.* **1984**, *259*, 11010.
(34) Warshel, A.; Sussman, F.; King, G. *Biochemistry* **1986**, *25*, 8368.
(35) Warshel, A.; Russell, S. *T. Q. Rev. Biophys.* **1984**, *17*, 283.
(36) King, G.; Warshel, A. *J. Chem. Phys.* **1989**, *91*, 3647.
(37) Lee, F. S.; Warshel, A. *J. Chem. Phys.* **1992**, *97*, 3100.
(38) Miertus, S.; Scrocco, E.; Tomasi, J. *Chem. Phys.* **1981**, *55*, 117.
(39) Miertus, S.; Tomasi, J. *Chem. Phys.* **1982**, *65*, 239.

Table 2. Results of the EVB/FEP Calculations with $\Delta G_0 = 5$ kcal/mol for the Nucleophilic Attack Step in the Reference Reaction[a]

set	time (ps)	ionization[c]	charge set[b]	starting geometry	$(\Delta\Delta G_{PT})^{w\rightarrow p}$	$(\Delta\Delta G_{nucl})^{w\rightarrow p}$	$(\Delta\Delta g^{\ddagger}_{nucl})^{w\rightarrow p}$	$(\Delta\Delta g^{\ddagger})^{w\rightarrow p}$
I	20	199, 327	1	relaxed	−3.9	12.5	−1.8	−5.7
II	20	199, 327	1	non-relaxed	−8.0	19.8	2.2	−5.8
III	40	199, 327	1	relaxed	−6.1	8.0	−2.9	−9.0
IV	20	199	2	relaxed	+4.8	−15.7	−11.5	−6.7
V	20	327	2	relaxed	+1.1	−6.1	−8.6	−7.5
VI	20	199, 327	2	relaxed	−2.4	−5.0	−8.5	−10.9
VII	20	all ion	2	relaxed	−5.2	−7.5	−7.3	−12.5
VIII	40	199, 327	2	relaxed	−3.7	3.5	−11.3	−15.0
IX	40	all ions	2	relaxed	−4.3	4.6	−7.7	−13.0

[a] Energies in kcal/mol, $(\Delta\Delta G_{PT})^{w\rightarrow p}$, $(\Delta\Delta g^{\ddagger}_{nucl})^{w\rightarrow p}$, $(\Delta\Delta G_{nucl})^{w\rightarrow p}$, and $(\Delta\Delta g^{\ddagger})^{w\rightarrow p}$ are respectively the reductions (upon transfer from water to enzyme) in the free energies of the proton transfer step, the nucleophilic attack step, the activation energy for the nucleophilic attack step, and the overall activation barrier. The calculations consider only the electrostatic contributions to the free energy using eqs 5 and 6. [b] Charge sets 1 and 2 designate respectively the simplified and ab initio charge set of Table 1. [c] All ion: all residues ionized within 15 Å from the substrate (Asp-72, Glu-199, Arg-289, Asp-326, Glu-327, Asp-397, Glu-443).

Table 3. Results of the EVB/FEP calculations with $\Delta G_0 = 0$ kcal/mol for the Nucleophilic Attack Step in the Reference Reaction[a]

set	time (ps)	ionization[c]	charge set[b]	starting geometry	$(\Delta\Delta G_{PT})^{w\rightarrow p}$	$(\Delta\Delta G_{nucl})^{w\rightarrow p}$	$(\Delta\Delta g^{\ddagger}_{nucl})^{w\rightarrow p}$	$(\Delta\Delta g^{\ddagger})^{w\rightarrow p}$
I	20	199, 327	1	relaxed	−3.9	+7.5	−6.4	−10.3
II	20	199, 327	1	non-relaxed	−8.0	+14.8	−2.6	−10.6
III	40	199, 327	1	relaxed	−6.1	+3.0	−4.6	−10.7
IV	20	199	2	relaxed	+4.8	−20.7	−10.7	−5.9
V	20	327	2	relaxed	+1.1	−11.1	−12.7	−11.6
VI	20	199, 327	2	relaxed	−2.4	−10.0	−10.8	−13.2
VII	20	all ion	2	relaxed	−5.2	−12.2	−10.6	−15.9
VIII	40	199, 327	2	relaxed	−3.7	−2.5	−8.9	−12.8
IX	40	all ion	2	relaxed	−4.3	−1.6	−9.6	−13.9

[a] Energies in kcal/mol, $(\Delta\Delta G_{PT})^{w\rightarrow p}$, $(\Delta\Delta g^{\ddagger}_{nucl})^{w\rightarrow p}$, $(\Delta\Delta G_{nucl})^{w\rightarrow p}$, and $(\Delta\Delta g^{\ddagger})^{w\rightarrow p}$ are respectively the reductions (upon transfer from water to enzyme) in the free energies of the proton transfer step, the nucleophilic attack step, the activation energy for the nucleophilic attack step, and the overall activation barrier. The calculations consider only the electrostatic contributions to the free energy using eqs 5 and 6. [b] Charge sets 1 and 2 designate respectively the simplified and ab initio charge set of Table 1. [c] 199, 327 indicate that Glu 199 and 327 are ionized. All ion: all residues ionized within 15 Å from the substrate (Asp-72, Glu-199, Arg-289, Asp-326, Glu-327, Asp-397, Glu-443).

energies were determined by a recent version of the Langevin Dipoles model that was specially parametrized for ab initio calculations of chemical processes in solutions.[40] In this way the free energy of the formation of the tetrahedral intermediate in water was estimated to be around 5 kcal/mol.

The EVB calculations were carried out using nine different simulation conditions which explored the effect of different factors. The calculation considers only the electrosatic contributions to the free energy, using the electrostatic mapping approach of eqs 5 and 6. The results of this comparative study are summarized in Table 2. This study considered two charge sets, the effect of the initial relaxation and the effect of protein ionizable groups. The study with the simplified charge set indicates that the initial relaxation effect can change the energy of the individual reaction steps but has a smaller effect on the overall reaction barrier. The effect of changing the simulation time from 20 to 40 ps was found to be significant, but further increase in the simulation time did not have a major effect. The change to the ab initio charge set (set 2) appears to increase the activation barrier to some extent. The overall activation barrier appears to be less sensitive to the simulation conditions than the energies of the individual steps. This behavior was also observed in early studies of serine proteases.[18]

In studying the effect of ionizable residues we focused on Glu-327 and Glu-199. To test the importance of ionization of further residues we also carried out simulations ionizing all residues within 15 Å from the substrate (Asp-72, Glu-199, Arg-289, Asp-326, Glu-327, Asp-397, Glu-443). This study did not attempt to determine the ionization state of distant residues (although this can be done, e.g. ref 23), but rather to establish a limit for the possible effect of these residues (this issue will be further discussed below). As Glu-327 and Glu-199 are around 6 Å apart and both interact with the same histidine residue their effect is coupled. The strongest coupling occurs at the transition state where Glu-199 repels the ionized oxyanion and attracts the protonated histidine. However, a unique analysis of the effect of mutation of any of these acids is not the subject of the present study. Regardless of the coupling issue it appears that when only one of the acids is ionized the catalytic effect is reduced significantly (see simulations IV and V with charge set 2). Neutralizing Glu-327 has a larger effect than neutralizing Glu-199 (this means that Glu-327 is more important for catalysis than Glu-199), but as we noted above these results have not been established in a quantitative way. The results obtained by ionizing both glutamates compared to ionizing all residues within 15 Å of the substrate show that the ionization of groups other than Glu-199 and Glu-327 does not contribute considerably to the catalysis (see simulations VI and VII with charge set 2). This indicates that negatively charged residues beyond the surface of the gorge do not contribute to the large value of k_{cat} in AChE. This finding is in full agreement with the available experimental observations.[41]

As the error in the calculations of ΔG_0 for the nucleophilic attack step is 2−5 kcal/mol, it is important to examine the sensitivity of the calculated activation free energy to this ΔG_0. Thus we compared the catalytic effect of the enzyme for two limiting values of ΔG_0 that were used in the parametrization of the reference reaction (see Table 3). The 5 kcal/mol change in exothermicity of the nucleophilic attack step resulted in a rather small (less than 1 kcal/mol) reduction of the $\Delta\Delta g^{\ddagger}$ values for the longer simulations. This indicated that the calculated catalytic effect is not crucially dependent on the exact energetics of the reference reaction. This is due to the fact that the catalytic effect reflects the difference between the reaction in protein and water (and is thus not sensitive to the absolute free energy).

(40) Florián, J.; Warshel, A. *J. Phys. Chem B* **1997**, *101*, 5583.
(41) Shafferman, A.; Ordentlich, A.; Barak, D.; Kronman, C.; Ber, R.; Bino, T.; Ariel, N.; Osman, R.; Velan, B. *EMBO J.* **1994**, *13*, 3448.

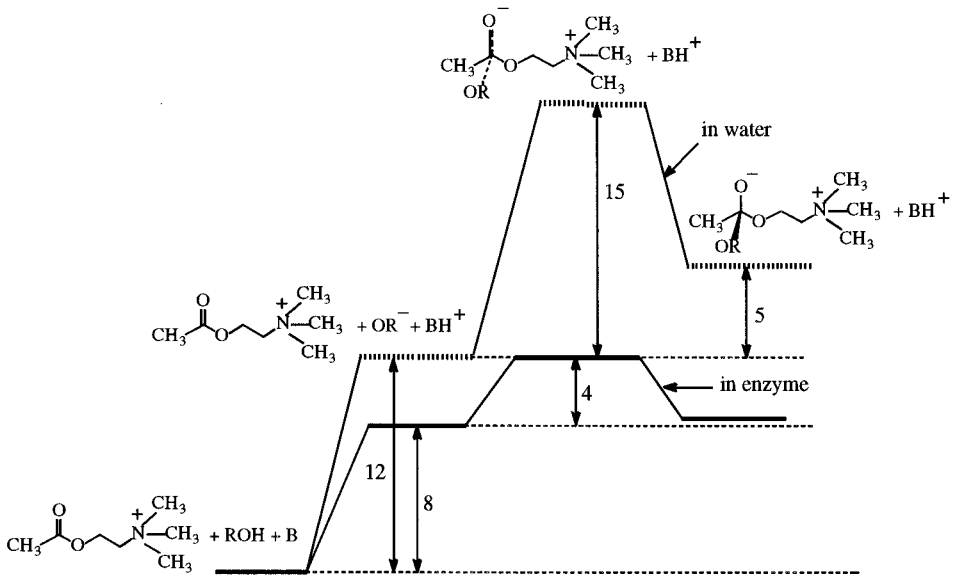

Figure 4. The calculated energetics of the acylation step of the acetylcholine hydrolysis in a solvent cage and in the enzyme active site. The figure summarizes in a schematic way the results of the EVB/FEP electrostatic mapping that corresponds to simulation VIII of Table 2.

Note, however, that since the reorganization energy is different for the reference reaction and the enzymatic reaction (see Section 3.4) we expect some effect of ΔG_0 on $\Delta\Delta g^{\ddagger}$.

The results of our 40-ps EVB/FEP electrostatic mapping calculations with charge set 2, with Glu-199 and Glu-327 ionized, are summarized in a schematic way in Figure 4 (the figure presents the free energies of the relevant EVB states rather than the actual free energy profile). As seen from the figure, the enzyme stabilizes both the proton transfer and the transition state of the nucleophilic attack relative to the corresponding steps in the reference reaction in water. The overall calculated stablilization is ∼15 kcal/mol, in a good agreement with the experimentally observed catalytic effect (the above mentioned $\Delta\Delta g^{\ddagger}$).

3.3 PDLD/S Calculations. To further examine the validity of our conclusions we also estimated the transition state energy using the PDLD/S method (see Section 2).

The binding energies of the ground and transition state were determined by using the substrate and the relevant fragment of the catalytic triad (represented in Figure 1) as "solute" atoms. The charges used were those of charge set 1 (see Table 1). The actual calculations of binding energies involved the generation of relaxed structures by MD simulations. The calculations were carried out with the simulation conditions summarized in Table 4. This study was less systematic and extensive than the EVB study and intended mainly to examine the electrostatic energies in configuration near the X-ray structure. All calculations with one exception gave a large reduction in $\Delta\Delta g^{\ddagger}$. The only exception is simulation set V, which involves a very weak protein constraint and ionization of all residues within 15 Å from the substrate. This problem reflects the difficulty of staying close to the original X-ray structure in simulations that include many ionized residues (note that with larger constraint we recover the catalytic effect). This important issue is usually addressed in our lab by balancing the overall charge of the system and having a larger simulation sphere. However, this is not so relevant to the present PDLD/S study, which focuses on the contributions to catalysis from configurations near the observed structure.

As can be seen from Table 4, we obtained a similar catalytic effect from ionization sets 1 and 2 while using a 0.3 constraint.

Table 4. The PDLD/S Activation Energy for the Acylation Step[a]

set	ionization[b]	const[c]	$\Delta\Delta g^{\ddagger}$
I	1	∞	−7.7
II	1	0.03	−10.4
III	1	0.3	−9.0
IV	2	∞	−12.5
V	2	0.03	−4.1
VI	2	0.3	−8.9

[a] $\Delta\Delta g^{\ddagger}$ was obtained from eq 6 while evaluating the relavent $\Delta G^{\ddagger}_{\text{bind}}$ and $\Delta G^{\circ}_{\text{bind}}$ by averaging the corresponding $\Delta\Delta G_{\text{bind}}$ over two configurations, each taken after 1 ps of simulation, using $\epsilon_p = 4$ and charge set 1. Energies in kcal/mol and contraints in kcal mol^{-1} Å^{-2}. [b] Ionization state 1 corresponds to the case where only Glu-199 and Glu-327 are ionized, while ionization state 2 corresponds to the case where all residues within 15 Å from the substrate are ionized (i.e., Asp-72, Glu-199, Arg-289, Asp-326, Glu-327, Asp-397, and Glu-443). [c] The indicated contraint (const) keeps the protein and substrate near their initial structures at the ground and transition state. These starting configurations were generated by running 5 ps simulations, using the EVB surfaces of the reactant state and the transition state.

This indicated that distant residues do not give a major contribution to catalysis.

4. The Origin of the Catalytic Power of AChE

Both the EVB/FEP and PDLD/S computational approaches reproduced the effect of the enzyme on the acylation step in a reasonable agreement with the experimentally-based estimate of section 3.1. The overall catalytic effect is associated with the stabilization of the transition state. In analyzing the catalytic effect it is sometimes convenient to describe this transition state stabilization in terms of the corresponding Marcus parabolas, where the reduction in the transition state free energy is expressed in terms of two parameters: (i) the free energy of the given step ΔG^0_{ij} and (ii) the reorganization energy, λ_{ij}, using the modified Marcus relationship[15]

$$\Delta g^{\ddagger}_{ij} \cong (\Delta G^0_{ij} + \lambda_{ij})^2/4\lambda_{ij} - \bar{H}_{ij} + (\bar{H}^2_{ij}/(\Delta G^0_{ij} + \lambda_{ij})) \qquad (12)$$

where $\bar{H}_{ij}$ is the average value of the off-diagonal EVB matrix element and the last term is usually small.

The catalytic effect associated with the change of ΔG^0_{ij} operates usually when charge separation is taking place in the

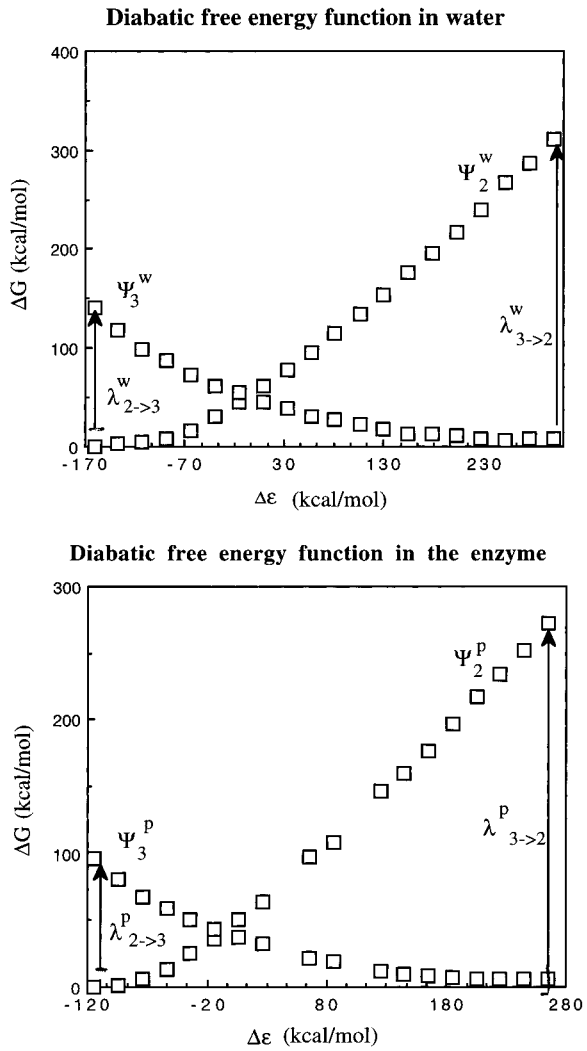

Figure 5. Diabatic free energy functions for the nucleophilic attack step in water (top) and in the enzyme (bottom). The relevant reorganization energies are indicated in the figure.

course of the reaction. In the present case we find that both ΔG^0_{12} (for the proton transfer step) and ΔG^0_{23} for the nucleophilic attack are reduced significantly. This effect involves major contributions from the two negatively charged glutamates (Glu-199 and Glu-327) that are involved in stabilizing the histidinium ion (His-440). The calculations also indicated that Glu-327 must be the key catalytic residue in the proton transfer step, but its effect cannot be investigated individually because of its strong coupling with Glu-199. This is also reflected by the results of the EVB/FEP simulations when both residues were ionized. The same stabilization effect that catalyzes the proton transfer step also helps in stabilizing the histidinium ion−oxyanion charge separated state in the course of the nucleophilic attack.

In addition to the reduction in ΔG^0_{ij} it is quite common to find that enzymes reduce the reorganization energies (λ_{ij}) (e.g., refs 16 and 42). This effect is related to the curvature of these surfaces, rather than the energy difference between their minima. In the present case it is found that reorganization energy plays an important role in the nucleophilic attack step. That is, as can be seen from Figure 5 (corresponding to simulation VIII) the reorganization energy in the enzyme is smaller by ∼40 kcal/mol than the corresponding energy in water. The easiest way to asses the corresponding effect is to consider the case where $\Delta G^0 \cong 0$ kcal/mol. In this case $\Delta g^{\ddagger} \cong \lambda/4 - H_{12}$, and a reduction of λ by 40 kcal/mol decrease the activation energy by 10 kcal/mol.

Although the above analysis clarifies that the enzymes reduce both ΔG^0 and λ it does not tell us anything about how this reduction has been accomplished. In fact, stating that ΔG^0 and λ were reduced is just another way of saying that $\Delta g^{\ddagger}$ is reduced. The fundamental question is, however, *how* ΔG^0 and λ are reduced. Previous studies[14,43,44] and the present one indicate that enzymes accomplish this task primarily by electrostatic effects. The remaining question is still how can an enzyme provide a larger electrostatic stabilization or "solvation" than water. The answer to this question has been given before.[15,43] It appears that the enzyme uses its folding energy to prepare a preorganized polar environment that does not have to pay a part of the reorganization energy needed to form such an environment at the transition state. This reorganization energy should not be confused with the reorganization along the reaction coordinate that is reflected by the λ of eq 12, although the two effects might be correlated. That is, the main effect of the preorganized environment is to reduce the ΔG^0 of high energy intermediates, but having the protein dipoles pointing at the optimal direction has the additional beneficial effect of reducing λ.

It must be pointed out in this respect that attempts (e.g. ref 45) to account for enzyme catalysis by invoking the small reorganization energy associated with charge transfer in nonpolar environment (i.e., $\epsilon < 4$) lead to anticatalysis. That is, since charged intermediates are unstable in nonpolar environments, ΔG^0 will increase and $\Delta G^{\ddagger}$ will become larger than smaller (see discussion in ref 42). Thus, the catalytic effect of the enzyme is associated with the small reorganization energy of its polar active site which is very different than any nonpolar environment.

Although this work focuses on the overall catalytic effect of the enzyme it is interesting to explore the effect of individual residues. A careful study along this line is quite demanding and out of the scope of the present work. Thus, we only considered several related issues in a very qualitative way. First, we examined the effect of distant ionized residues (all residues except Glu-327 and Glu-199) by using the non-relaxed PDLD/S approach with $\epsilon_{in} = 40$ (section 2.2). It was found that none of these residues contributes to catalysis more than 0.5 kcal/mol. This finding is in agreement with mutation studies.[41] The effect of nearby ionized residues cannot be studied by the non-relaxed PDLD/S approach and the relevant EVB results will be considered below. Similarly, the effect of polar side chains is not expected to be reproduced in a reliable way without costly consideration of the reorganization of the relevant dipoles during the reaction. The only group contributions (except those of distant ionized residues) which are expected to be captured reliably by the non-relaxed approach are the contributions of the main chain dipoles. The corresponding calculations are summarized in Figure 6. According to these calculations the most significant contribution that appears to persist in calculations with different conditions is due to the main chain effect of residues Gly-118, Gly-119, and Ala-201. The amide nitrogens of these residues are located 2.9, 2.9, and 3.2 Å from the carbonyl oxygen of the acetylcholine, and they participate in

(42) Yadav, A.; Jackson, R. M.; Holbrook, J. J.; Warshel, A. *J. Am. Chem. Soc.* **1991**, *113*, 4800.
(43) Warshel, A. *Proc. Natl. Acad. Sci. U.S.A.* **1978**, *75*, 5250.
(44) Warshel, A.; Åqvist, J. *Annu. Rev. Biophys. Biophys. Chem.* **1991**, *20*, 267.
(45) Krishtalik, L. I. J. *Theor. Biol.* **1980**, *86*, 757.

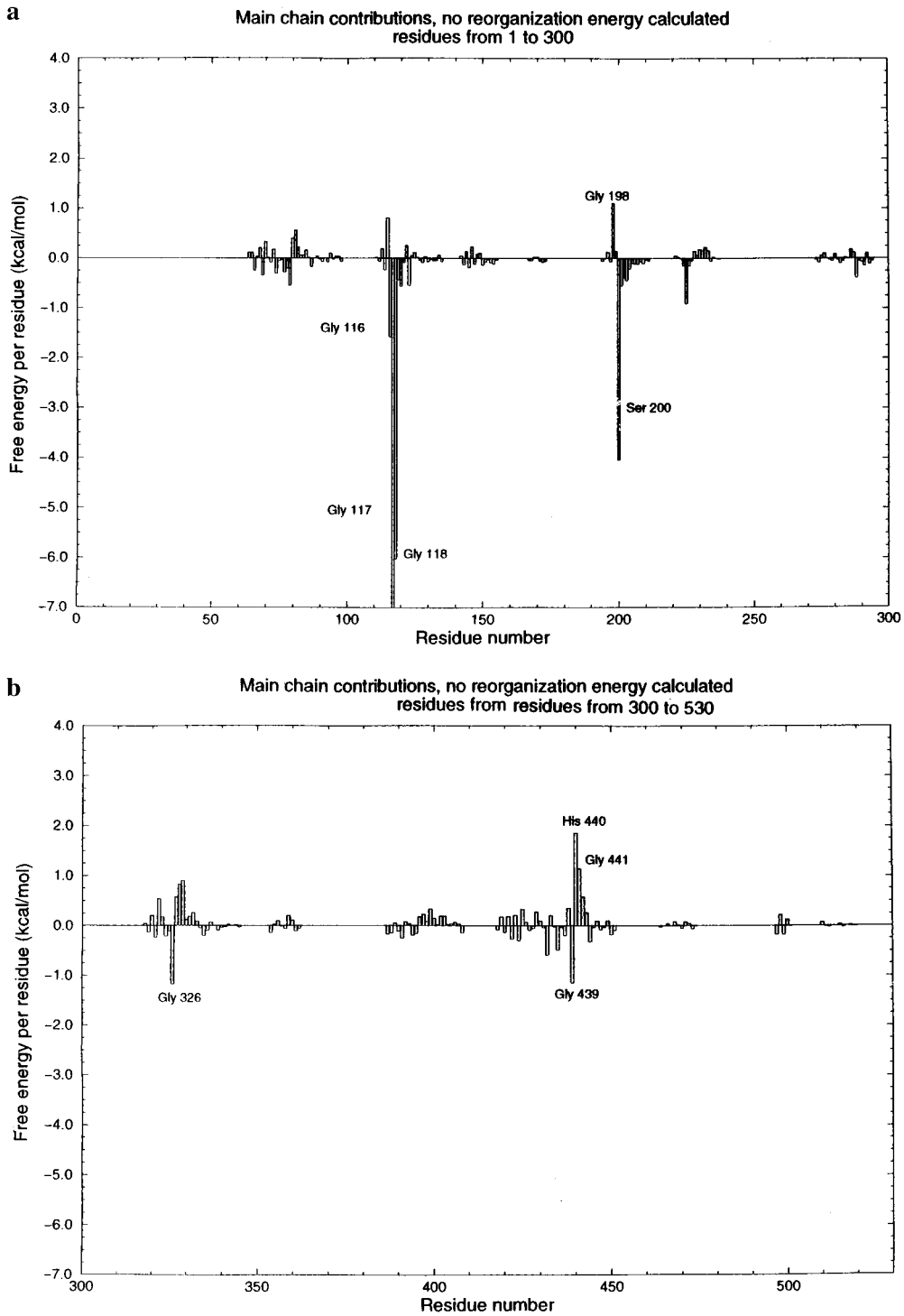

Figure 6. Main chain contributions to catalysis obtained by the non-relaxed PDLD/S method with $\epsilon_{in} = 4$ (residues 1−300 (a), residues 300−530 (b)).

forming the oxyanion hole that stabilizes the transition state by the preoriented dipoles of these residues.

While distant ionized residues appear to have a small effect that could be explored using the non-relaxed approach with large ϵ_{in}, the effect on nearby ionized residues requires more careful attention. The EVB calculations summarized in Tables 2 and 3 can be used to estimate the catalytic contributions of Glu-327 and Glu-199. The corresponding energetics can be obtained by considering the same simulation conditions and comparing the effect of having both 199 and 327 ionized as opposed to only having 327 ionized. Using Table 3 for this comparison suggests that the effect of mutating 327 and 199 to uncharged residues should be respectively around $(-5.9 + 13.2) = 7.3$ and $(-11.6 + 13.2) = 1.6$ kcal/mol. Alternatively, the use of Table 2 gives 4.2 and 3.4 kcal/mol for these two mutations. One should note, however, that we only report here qualitative results and that more reliable estimates would require longer simulations. Furthermore, it is also useful to note that mutation studies by FEP approaches tend to overestimate charge−charge interactions (e.g. see ref 46). At any rate, accepting the present results as a qualitative guidance, we conclude that the contribution of Glu-327 to catalysis is larger than that of Glu-199. The

(46) Alden, R. G.; Parson, W. W.; Chu, Z. T.; Warshel, A. *J. Am. Chem. Soc.* **1995**, *117*, 12284.

reason for the small contribution of Glu-199 is the repulsion between the negative charge of this group and the negative charge that resides on the oxyanion at the transition state. This is consistent with the surprising results of the kinetic data of the E199Q mutant, which showed only a 5-fold decrease in k_{cat} compared to the wild-type enzyme.

An issue that is frequently addressed in studies of AChE is the role of the hydrophobic residues on the surface of the gorge that leads to the catalytic triad. There has been much discussion about aromatic guidance of the substrate in the diffusion controlled reaction.[2,47] Recently it was suggested[5] that the hydrophobic environment provided by AChE, similar to that of the gas phase, is more favorable for the formation of the tetrahedral adduct (formed in the course of nucleophilic addition on carbonyl compounds) than the aqueous solution. Such gas-phase-like catalytic proposals or the basically equivalent idea that enzymes work by desolvation effects using hydrophobic active sites has been frequently advanced.[48−51] However, our previous works[52] have established that this effect is in general anticatalytic. That is, as long as the enzyme has to reduce k_{cat}/k_M it must reduce the energy of the transition state relative to that of the E + S state. Destabilizing the ES state cannot help in this way. Furthermore, if the transition state is ionic it will be destabilized in a nonpolar environment. The confusion that led to the popularity of the desolvation proposal is associated with the use of incorrect thermodynamic cycles (see ref 52) and neglecting the energy of forming ionic reactants in hydrophobic environment or in moving such reactants from water to hypothetical nonpolar active sites. To illustrate this problem in the case of AChE we used the PDLD/S approach to calculate the transition state binding energy in a totally nonpolar enzyme. It was found that the nonpolar enzyme destabilizes the transition state relative to the reactant by 11.4 kcal/mol compared to water. This would mean that a nonpolar enzyme would lead to anticatalysis rather than catalysis of the acetylcholine hydrolysis, which is certainly inconsistent with the experimental estimate of the enormous increase in k_{cat} relative to the corresponding rate constant in the reference reaction in water.

An interesting and insightful issue is associated with the effect on nonpolar residues on k_{cat}/K_M rather than k_{cat} alone. That is, hydrophobic residues which are far from the region where chemical transformation occurs can contribute significantly to binding of both the ground and the transition state leading to an overall stabilization of the TS relative to the E + S state. A candidate for such an effect is tryptophan 84, which interacts directly with the ammonium moiety and is known to have a significant effect on K_M. To examine the role of this residue we evaluated the effect of the W84A mutant using the PDLD/S model. The calculations resulted in a 4−5 kcal/mol reduction in the binding energy of the TS, which corresponds to an increase of about $\sim 10^3$ in k_{cat}/K_M. On the other hand k_{cat} remains unchanged. This corresponds nicely to the observation[8] that this mutant reduces k_{cat}/K_M by $\sim 3 \times 10^3$ while changing k_{cat} by only a factor of $\sim$5. Interestingly, the calculated effect appears to be associated with the permanent dipole of the tryptophan (the $V_{Q\mu}$ of eq 7) rather than with its induced dipoles. Regardless of the actual reason it is interesting that the ground state is stabilized rather than destabilized. This is an example of the fact that enzymes catalyze reactions by stabilizing the transition state rather than destabilizing the ground state.[15] As shown here, it is possible to increase k_{cat}/K_M by stabilizing the nonreactive parts of the substrate and reducing K_M, but this is done by stabilizing both the ground and the transition state to a similar extent. This is an instructive point in view of the frequently accepted Jencks' proposal[53] that enzymes work by ground state destabilization. That is, Jencks' pioneering work recognized the fact that an enzyme, must provide a strong binding in order to increase k_{cat}/K_M, but suggested that k_{cat} is

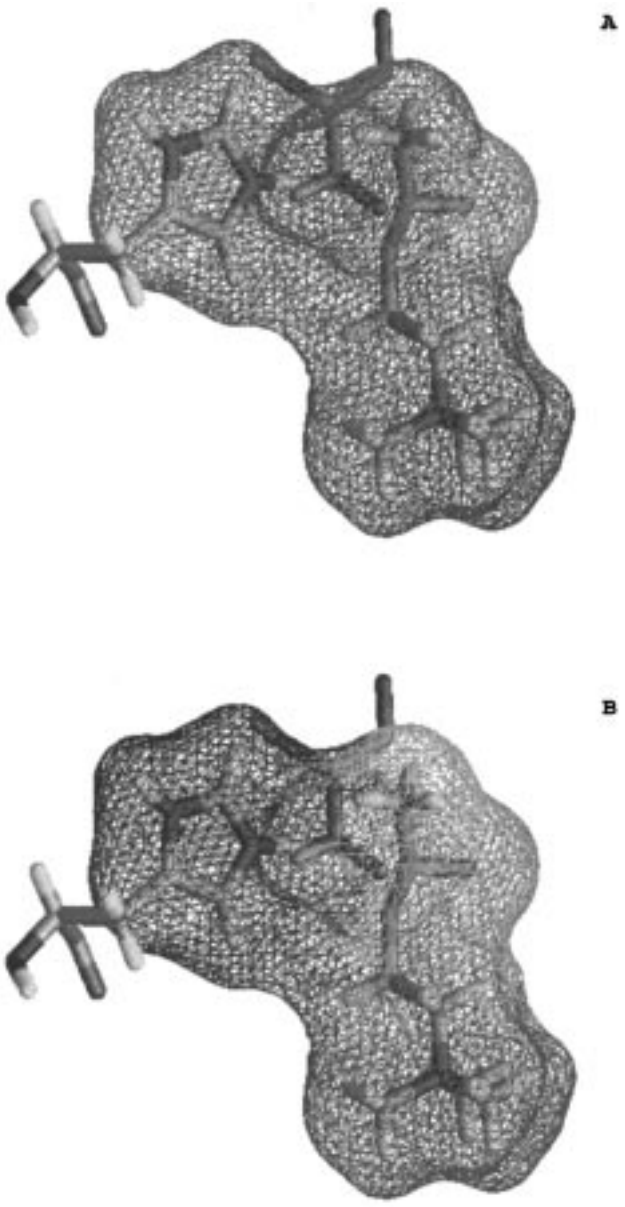

Figure 7. Comparing the electrostatic potential on the transition state dipole (the dipole formed by $His^+-oxyanion^-$) due to the surrounding environment (water (A) and protein (B)). The dark and light regions correspond to negative and less negative (or positive) potentials, respectively. The figure illustrates that the transition state dipole is stabilized more in the protein than in water. That is, in water, the potential on the $oxyanion^-$ is only slightly less negative than on His^+ (this is not seen clearly in a black and white drawing. On the other hand, in the protein we have a negative potential on His^+ and a positive potential on the $oxyanion^-$.

(47) Rosenberry, T. L.; Neumann, E. *Biochemistry* **1977**, *16*, 3870.
(48) Cohen, S. G.; Vaidya, V. M.; Schultz, R. M. *Proc. Natl. Acad. Sci. U.S.A.* **1970**, *66*, 249.
(49) Wolfenden, R. *Science* **1983**, *222*, 1087.
(50) Dewar, M. J. S.; Dieter, K. M. *Biochemistry* **1988**, *27*, 3302.
(51) Lee, J. K.; Houk, K. N. *Science* **1997**, *276*, 942.
(52) Warshel, A.; Åqvist, J.; Creighton, S. *Proc. Natl. Acad. Sci. U.S.A.* **1989**, *86*, 5820.
(53) Jencks, W. P. *Catalysis in Chemistry and Enzymology*; Dover: New York, 1987.

increased by ground state destabilization effects. This proposal clearly has a problem for enzymes that evolved under the constraint of increasing k_{cat}/K_M rather than k_{cat} (this constraint applies to many enzymes in their current stage in evolution). In any case, any ground state destabilization effect that keeps the transition state energy constant would not change k_{cat}/K_M and thus has no evolutionary advantage (see ref 15). More specifically, residues that contribute to k_{cat}/K_M in a major way appear to do so by stabilizing the ground state and transition state to the same amount. On the other hand, residues that only change k_{cat} (e.g., Glu-327) appear to do so by transition state stabilization rather than ground state destabilization.

Although the present study did not involve a systematic examination of the effect of different mutations it led to the following conclusions: (i) dipolar residues help in direct stabilization of the transition state; (ii) nearby ionized residues and in particular Glu-327 help in catalysis; (iii) distant ionized residues do not contribute in a major way; and (iv) k_{cat} is not increased by desolvation effects and the catalytic effects of hydrophobic residues are associated with the binding of parts of the substrate that are far from its reacting region.

The overall catalytic effect is associated with electrostatic stabilization of the transition state. This is done by providing the electrostatic potential that is complementary to the dipolar charge distribution of the (His^+−$oxyanion^-$) transition state (see Figure 7). The effectiveness of this electrostatic potential appears to be associated with the preorganization of the polar environment of the active site.

It might be useful to conclude this paper by discussing a possible perception that the present conclusions are not new and that our model does not tell one how to refine earlier results or to formulate testable hypotheses. In addressing such concerns we start by restating that the observed effect of different mutations cannot tell us about the *overall* catalytic effect (see Section 1) and such effects can be interpreted in different ways. Furthermore, mutation experiments *cannot tell us* what is the actual effect of the oxyanion hole since this crucial catalytic element involves main chain dipoles. In our opinion and experience, the best way of arriving at a unique interpretation of mutation effects is to use computer modeling approaches (see discussion in ref 54). For example, the analysis of the same mutations considered in this work (without the use of computer simulations in evaluating the totality of the effect of the enzyme) led previous workers to propose that the enzyme works by desolvating the transition state. Our computer modeling, on the other hand, led to the opposite conclusion. As to presenting testable hypotheses, the current work and many of our early studies advanced repeatedly the "hypothesis" that enzymes work by providing electrostatic stabilization to the corresponding transition states and that this is associated with the preorganized polar environment.[43] This view has been confirmed by computer modeling of different enzymes (e.g., ref 15). Thus, the best way of verifying or modifying our picture should probably involve more refined computer modeling. Of course, experimental studies are crucial for providing new observations that should be reproduced by the simulations (before the simulations are considered useful for studying the overall catalytic effect). However, any credible interpretation of such experiments in complex systems must involve some type of structure−function correlation, and this is best done by computer modeling. As to the suggestion for new experiments, one may try to find support for the desolvation hypothesis (that was eliminated in the present work) by mutating nonpolar active site residues to polar residues and examining the resulting changes in k_{cat}. However, the interpretation of such experiments cannot be performed in a unique way without a proper computer model. Thus, we believe that true understanding of enzyme catalysis requires models capable of reproducing the *total* catalytic effect.

Acknowledgment. M. F. thanks the support of Eötvös Fellowship of the Hungarian Government and the SOROS Foundation and Dr. Ingo Muegge and Dr. Jorg Bentzien for helpful discussions. A part of this work was supported by NIH Grant No. GM-24492.

JA972326M

(54) Warshel, A.; Naray-Szabo, G.; Sussman, F.; Hwang, J.-K. *Biochemistry* **1989**, *28*, 3629.
(55) Warshel, A. *J. Phys. Chem.* **1979**, *83*, 1640.